CW-POWERED SQUEGGING MICROMECHANICAL CLOCK GENERATOR

Ruonan Liu, Jalal Naghsh Nilchi, and Clark T.-C. Nguyen
University of California at Berkeley, Berkeley, CA, USA

ABSTRACT

A mechanical circuit has been demonstrated that harnesses squegging to convert -50dBm of input continuous-wave (CW) energy into a local 1-kHz clock output while consuming three orders less local battery power than a typical real-time clock (RTC). Unlike a previous clock receiver that relied on a modulated RF input, this clock generator converts a CW input—no modulation needed—to a clock output via squegging of an impacting micromechanical resonant switch ("resoswitch"). Here, impact-induced disruption compels the device's resonating element to lose oscillation amplitude (hence stop impacting), then recover to impact again, only to again lose amplitude, in a periodic and repeatable fashion. The resulting time domain waveform, with periodic peaks and valleys, then provides a stable frequency that serves as a local on-board clock for low data rate applications. By dispensing with the need for a positive feedback sustaining amplifier, this CW-powered mechanical clock generator operates with only 0.8nW of battery power when outputting a triangle-wave into 0.8pF, which is 1250× lower than the 1μW of a typical RTC.

INTRODUCTION

The vast majority of electronics utilize RTCs to keep time for numerous purposes, from time stamping, to computational synchronization, to event synchronization, e.g., simultaneous waking of sensors in a network. Since RTCs generally operate continuously to keep time, it is paramount that they be power efficient, especially when used in battery-operated devices. The typical RTC consumes 1μW of power, which is sufficiently low for devices equipped with coin cell batteries. It is not low enough, however, for the large-scale sensor networks of the future, envisioned by many to employ massive numbers of sensor nodes, each of which must cost very little, so might rely on cheap printed batteries storing only 1J of energy. If such a sensor network uses a sleep/wake scheme to minimize power, then often the RTCs set the bottleneck on sensor node lifetime. For 1J of energy to last 1 year in a sensor node, its RTC must consume less than 32nW.

To solve this problem, previous work introduced an RF-powered micromechanical clock generator [1] that dispenses with the conventional transistor-based positive feedback oscillator approach to successfully reduce power consumption down to 34nW. As shown in Figure 1, this previous micromechanical clock generator manifests as an all-mechanical receiver [2] that detects and demodulates RF input energy via a resoswitch device [1]. The resoswitch comprises a polysilicon movable shuttle suspended by stress-relieving folded-beams, flanked by capacitive-comb transducers, and employing sharp metal protrusions to impact the indicated output

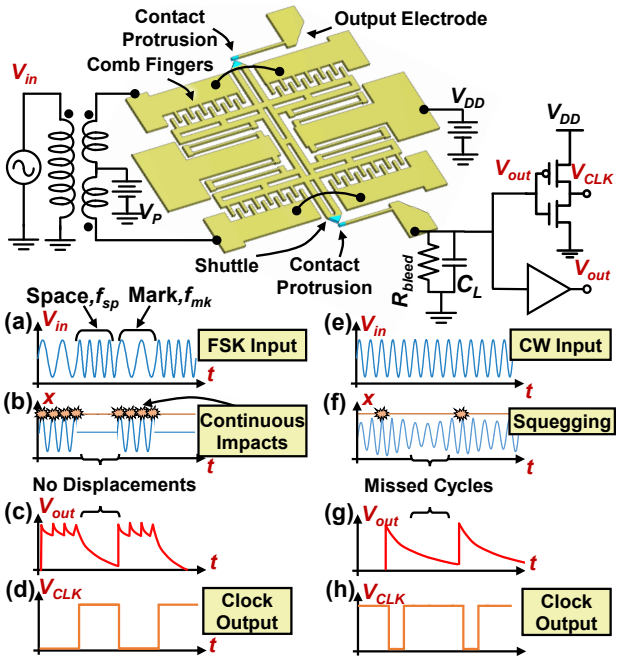

Figure 1: Illustrations summarizing operation of FSK- and CW-powered MEMS clock generators in a typical operating circuit. (a)-(d) summarize FSK-powered operation, where (a) an input FSK signal drives the resoswitch to (b) impact on the mark frequency and not on the space frequency. Rectification by C_L and R_{bleed} then produces the (c) trapezoidal waveform, which an optional inverter converts to (d) a square clock output. (e)-(h) summarize a CW clock generator, where (a) a CW input at resonance drives the resoswitch to (b) squegging, which with rectification produces (c) a rising edge triangle waveform suitable for clock use.

electrodes. Once driven to resonance at a sufficiently large amplitude, the shuttle protrusion impacts the output electrode, closing a switch contact and delivering charge from the supply V_{DD} to the output load capacitor C_L, charging it to V_{DD}. The resoswitch in the previous FSK clock generator operates in an OOK fashion, where a mark input frequency f_{mk} excites resonance impacts to generate voltage spikes at f_{mk} that are rectified by R_{bleed} and C_L to yield a clock "high". Meanwhile, an off-resonance space frequency f_{sp} induces no motion, so no impacts, allowing C_L to discharge via R_{bleed}, generating a clock "low". And all with extremely low power consumption.

One drawback of the previous clock generator is the need for a clock-modulated RF waveform. For example, one target application scenario where all RTCs receive clock activation energy wirelessly would be easier to implement if the energy powering the clocks need not be modulated, i.e., if it could be delivered as a simple continuous-wave (CW) tone. Pursuant

to enabling this, the mechanical clock demonstrated here explores the use of squegging to convert -50dBm of input CW energy into a local 1-kHz clock output while consuming only 0.8nW of battery power when outputting a triangle-wave into 0.8pF, which is 1250× lower than the 1µW of a typical RTC.

CW CLOCK GENERATOR

Except for use of a W/TiN contact protrusion metal instead of Au (for reasons to be described), the structure of the CW clock generator mimics that of the previous FSK one. Its operation, on the other hand, is quite different. Instead of functioning as a receiver that faithfully demodulates a received clock signal, the CW clock generator effectively 1) harvests the energy from a remote unmodulated CW input signal; then 2) uses the energy to instigate and facilitate generation of a stable clock signal from a local power source.

The ability to generate a stable clock output derives not from reception of a specific modulated signal, but rather from "squegging" resonance impact dynamics [3]. To explain, Figure 1 illustrates the overall operation of the CW clock generator. As with the FSK-input version summarized in (a)-(d), the CW-input version receives energy via v_{in}, but this time as (e) an unmodulated continuous waveform (that could be wireless) within the response bandwidth of the shuttle. This input induces a force at resonance, which in turn instigates resonance vibration of the shuttle, with an amplitude that grows until the shuttle impacts the output electrode(s). Upon each impact, current flows from the battery supply V_{DD} to the output load capacitor C_L, quickly charging it to V_{DD}.

At this point, if the shuttle continues to impact the output electrode, C_L remains charged to V_{DD}, which means there is no periodic clock signal. A clock signal, of course, requires that C_L charge and discharge periodically. R_{bleed} in Figure 1 is poised to discharge C_L at a designed "bleed" rate, but only if impacting stops. The present clock generator realizes cessation of impacting by designing the resoswitch to squegg at a specific clock frequency.

Figure 1(f) illustrates the squegging phenomenon where impact-induced disruption compels the device's resonating element to lose oscillation amplitude (hence stop impacting), then recover to impact again, only to again lose amplitude, in a periodic and repeatable fashion. The resulting time domain waveform, with periodic peaks and valleys, then provides a stable frequency that can then serve as a local on-board clock for low data rate applications.

SQUEGGING BY DESIGN

The resonance force response simulations in Figure 2(b) and (c) more fully explain the mechanism behind squegging by comparison with the non-impacting (so non-squegged) case in (a). With no impacts, the amplitude of the resonant structure grows until limited by (gentle) loss, at which point it reaches steady-state vibration, where its displacement phase lags that of the input excitation force by 90°. In contrast, when a nearby electrode limits the displacement amplitude, energy absorption upon contact imposes a phase delay $\Delta\varphi$ on shuttle bounce-back, which then lowers the efficiency

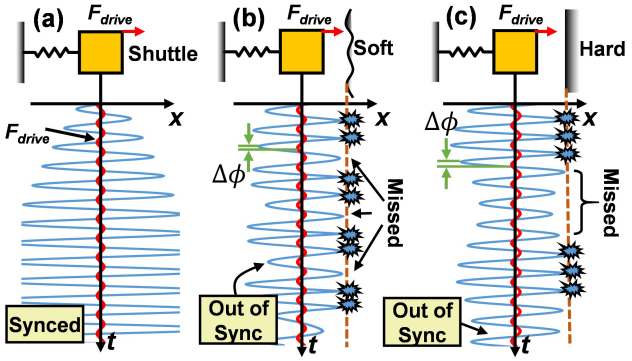

Figure 2: Simulated transient waveforms showing (a) no impacts, (b) small phase shifts Δφ for soft impacts, and (c) large Δφ for harder impacts. Here, phase shifts pull the resoswitch out of sync with the drive force, reducing its efficiency and thereby causing squegging where no impacts occur over the next few cycles until the structure re-synchronizes with the input force and recovers to impact once again.

of the input drive, resulting in a smaller subsequent amplitude in the next cycle [5]. The amount of phase shift, and thus number of missed cycles, depends strongly on the hardness of the contact: For the case of a soft contact, as in (b), $\Delta\varphi$ is small, so very few cycles miss, and very little squegging ensues. A hard contact, on the hand, depicted in (c), imposes much larger dephasing that results in many missed cycles, giving R_{bleed} enough time to discharge C_L. Again, the resoswitch of the present CW clock generator differs from that of the previous FSK one in its use of a harder W/TiN contact interface, which enhances squegging. Ultimately, the system recovers to a state where the displacement is again 90° phase-shifted from the input force, raising the drive force efficiency to grow the displacement amplitude to again impact, after which the cycle repeats. The stability of the cycle determines the ultimate stability of the clock.

As described in [5], there are numerous knobs by which squegging and its periodicity can be controlled, including gap distance, drive symmetry, Q, contact hardness (as governed by contact interface materials), and drive strength. Inevitably, each of these knobs governs the squegging period by influencing contact dynamics.

To address contact dynamics, consider that before making contact with the electrode, the resonator experiences only the drive force F_{drive}. Upon impact, the impacting electrode applies a counteracting contact force F_c on the resonator to prevent it from penetrating into the electrode. The relevant equations are:

$$F_c = k_x(x_1 - x_0) \quad (1)$$

$$m_1\ddot{x_1} + b\dot{x_1} + kx_1 = F_{drive}\ (x_1 < x_0) \quad (2)$$

$$m_1\ddot{x_1} + b\dot{x_1} + kx_1 = F_{drive} - F_c\ (x_1 \geq x_0) \quad (3)$$

where x_1, m_1, k and b are the displacement, equivalent mass, stiffness and damping factor of the resonator, respectively. x_0 is the initial spacing between the resonator and the output electrode, i.e., the displacement threshold to be overcome before the resonator shuttle makes initial contact.

The contact force is a product of the penetration depth

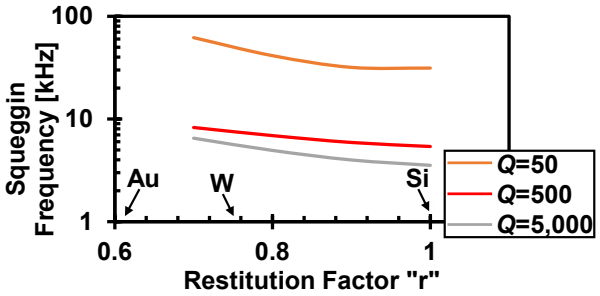

Figure 3: Plots showing how electrode hardness ("r"factor) and system Q influence squegging frequency.

and the contact stiffness k_c, the latter of which increases with penetration depth. For the specific design here, the hard surface of the W/TiN contact material dictates very shallow penetration, which means k_c is approximately constant over the period of contact. However, since the value of k_c depends on many other factors, such as the contact velocity v_1, the surface roughness, and the mechanical stiffness of the electrode [4], it often takes the form of a fitting factor to satisfy the penetration tolerance [6].

Pursuant to facilitating study of how impacts influence the squegging frequency, one can introduce a post impact shuttle velocity v_1', defined as [7] $v_1' = rv_1$ where r is a coefficient of restitution [8] that captures impact conditions and that increases with increasing hardness [9]. A positive r means the impact does not invert the direction of the resonator's velocity, which means the resonator suffers a smaller phase setback $\Delta\varphi$ than impacting with a negative r factor. After each impact at time t_n, the initial conditions of differential equations (2) and (3) change to:

$$x_1(t_n) = x_0 \quad (4)$$

$$v_1(t_n^-) = rv_1(t_n^+) \quad (5)$$

where t_n^- and t_n^+ are the times before and after the nth impact at t_n, respectively. The effect of these initial conditions fade out as $e^{-\left(\frac{\omega}{2Q}t\right)}$, which means the displacement phase lag recovers with a time constant $\tau \sim 2Q/\omega$. Thus, the higher the Q, the longer it takes to recover, the more missed impacts, the longer the discharging period, and the lower the output squegging frequency. Figure 3 simulates squegging frequency as a function of r for different Qs.

MATERIAL DESIGN AND FABRICATION

Given its time-keeping function, the frequency of the CW clock generator should be low, which suggests its resonator element have high Q and its contact interface be hard. To insure high resonant Q, the resoswitch for CW clock generation uses polysilicon structural material to set elastic properties, while employing hard W/TiN metal (for long missed impact periods) only in areas where impacting contacts occur.

Figure 4 presents the fabrication process flow. The process starts with a 4μm LPCVD of sacrificial oxide followed by lithographic patterning using a negative structure mask and a timed etch to remove 2 μm of the oxide, leaving a mold (*cf.* Figure 4(a)) to shape a subsequent *in situ* phosphorous-

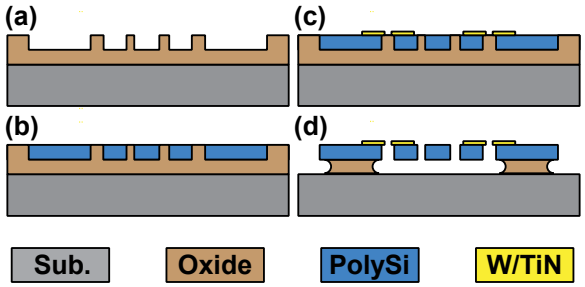

Figure 4: Fabrication process flow for the polysilicon resoswitch with W/TiN contact tips.

doped polysilicon deposition to the desired structural geometry. Next, CMP planarizes the surface leaving the polysilicon flush with the oxide mold (*cf.* Figure 4(b)). This facilitates subsequent formation of metal impact contacts, for which 150nm of W followed by 20nm of TiN are sputtered and etched to the contact protrusion geometries, which cover only areas near the contact points. The majority of the resonator structure, especially its folded-beam supports, remain metal free, so retain their very high Q.

The metal etch recipe comprises two steps: first, an SF_6 plasma etch to cut through the TiN protective layer above W; then, a wet etch in H_2O_2 solution using the TiN as a mask to remove the remaining W. The wet etch leaves the polysilicon beneath intact, preserving its Q. Finally, a timed wet etch in 49% HF with galvanic corrosion-suppressing anti-oxidant releases the structure while leaving the anchor areas attached to the substrate (*cf.* Figure 4(d)). Note that it is actually the portions of W/TiN protruding beyond the polysilicon edges that actually make switch contact. Figure 5(a) shows a scanning-electron micrograph (SEM) of the released structure.

EXPERIMENTAL RESULTS

The fabricated resoswitches were wirebonded onto a printed circuit board (PCB) and emplaced into a custom-built bell jar to provide a 100μTorr vacuum test environment and allow SMA connection to external test instrumentation that include voltage sources and an oscilloscope.

Figure 5(b) presents the measured frequency response of a non-impacting resoswitch, showing a vacuum-Q of 32,625, which is 23× higher than the previous resoswitch of [4], enabled largely by the use of anti-oxidant during HF release.

Figure 6 presents measured waveforms at various points labeled in the Figure 1 circuit. As shown, the -50dBm CW input signal of (a) drives the resoswitch to impacting, but with squegged behavior, where impacts do not occur on all cycles, as indicated by the varying amplitudes in Figure 1(b) and (c). Thus, impact-based charging of the output capacitor C_L occurs only at the beginning of a squegging cycle, after which C_L discharges through bleed resistor R_{bleed}, inevitably generating the triangle waveform shown with a frequency of 1kHz determined by resoswitch design.

To characterize the stability of the clock, Figure 7 presents the measured Allan deviation for the triangle waveform of Figure 1(b) that reaches 10^{-3}. This is stable enough for low-end commercial applications, such as timers for washing

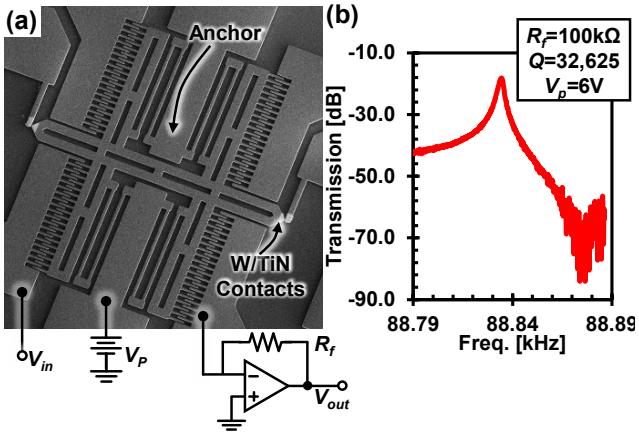

Figure 5: (a): SEM of a fabricated CW-powered clock generator resoswitch with W/TiN contacts. (b): 100μTorr-measured non-impacting frequency spectrum for the device.

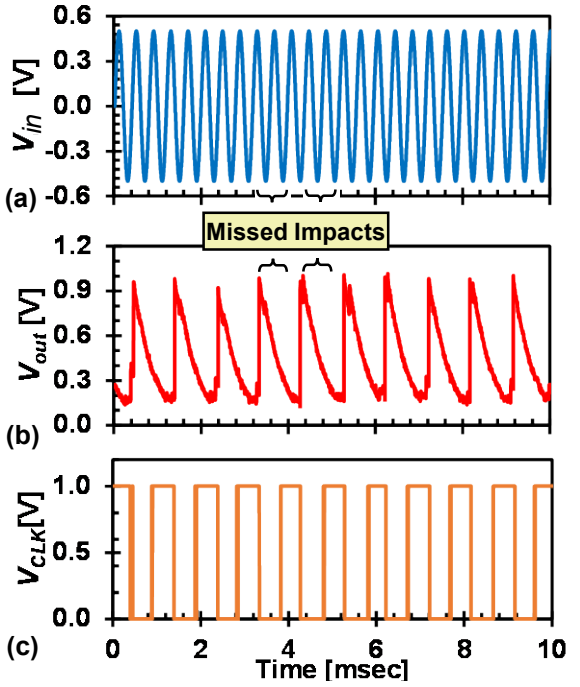

Figure 6: Measured waveforms for the CW-powered MEMS clock depicted in Fig.1. (a) Input CW waveform V_{in} at the resoswitch resonance frequency. (b) Squegged raw output waveform V_{out} across load capacitor C_L. (c) V_{CLK} at the output of the optional inverter.

machines and low data rate wireless sensors. Addition of a single inverter provides a cleaner square-wave signal (*cf.* (c)), but is actually not needed for rising edge-triggered systems.

In Figure 1, the output node of the resoswitch connects via wirebond to two separate following stages: a buffer (Texas Instruments THS4271) that feeds the oscilloscope; and an inverter that produces the square wave clock output. The total capacitive load presented to the resoswitch output thus combines 0.8pF of buffer input capacitance, 10pF of inverter input capacitance, and 7.5pF of internal chip capacitance, for a total of 18.3pF. With V_{DD} of 1V and clock frequency f_{CLK} of 1kHz, the total power consumption is 18.3nW.

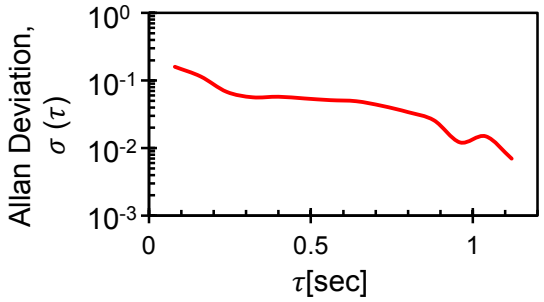

Figure 7: Measured Allan deviation for the resoswitch clock generator powered by a −50dBm CW resonance input.

Without the inverter, when outputting a triangle wave into only the 0.8pF input capacitance of the buffer, the clock only consumes 0.8nW, which is 1250 times lower than the 1μW of a typical RTC!

CONCLUSION

With its ability to use energy from a simple CW wave, with no modulation required, the demonstrated mechanical CW clock generator potentially enables scenarios where even the simplest inexpensive products, e.g., toys, paper, can benefit from an embedded clock that might be key to smart operation as long as CW energy is available. Considering that radio signals are everywhere, even in remote areas (e.g., WWVB, AM), the prospects of this technology making available clocks that can permeate simple products is not as outlandish as one might think at first glance. Still, there is much work to be done to improve the stability and accuracy of this clock, especially against changing environmental conditions. Improved modeling and understanding of squegging has already uncovered promising solutions to these problems that make for some interesting research ahead.

ACKNOWLEDGEMENTS

This work is funded by the DARPA N-ZERO program.

REFERENCES

[1] R. Liu, *et al*, "RF-Powered …," *IFCS*, New Orleans, 2016, DOI: 10.1109/FCS.2016.7546785.
[2] R. Liu, *et al*, "Zero …," *Transducers*, Anchorage, 2015, DOI:10.1109/TRANSDUCERS.2015.7180878.
[3] S. Shaw *et al*, "A Periodically …," Journal of Sound and Vibration, 1983, DOI:10.1016/0022-460X(83)90407-8.
[4] R. Liu, *et al*, "Soft-Impacting ...," *MEMS*, Shanghai, China, 2016, DOI: 10.1109/MEMSYS.2016.7421555.
[5] Y. Lin, *et al*, "Polycide …," *MEMS*, San Francisco, 2014, DOI: 10.1109/MEMSYS.2014.6765881
[6] ANSYS, "ANSYS Simulator Training Manual," 2005.
[7] C. Budd, *et al*, "Chattering …," Philosophical Transactions of …, 1994, DOI: 10.1098/rsta.1994.0049.
[8] C. Budd, *et al*, "The effect of …," Journal of Sound and Vibration, 1995, DOI:10.1006/jsvi.1995.0329.
[9] R. L. Jackson, *et al*, "Predicting …," Nonlinear Dynamics, 2010, DOI: 10.1007/s11071-009-9591-z.

CONTACT: Liu, R, liur@eecs.berkeley.edu